PLASMA DIAGNOSTICS IN ITER CONTROL

G. Vayakis, D. Boucher, N. Bretz,[a] A. Costley, Y. Gribov,[b] L. deKock,

G. Janeschitz,[c] L. Johnson, C. Kessel,[a] V. Mukhovatov, A. Portone,[b] J. Wesley,

and the ITER Joint Central Team and Home Teams

ITER JCT, San Diego JWS, 11025 N. Torrey Pines Rd, La Jolla CA 92037, USA.
[a] Princeton Plasma Physics Laboratory, New Jersey, USA
[b] ITER JCT, Naka JWS, Naka, Japan
[c] ITER JCT, Garching JWS, Garching, Germany

1. Introduction

A full complement of diagnostics is planned for ITER [1]. These will support a variety of measurements, classified according to their major role as those that are required for machine protection and plasma control (group 1a); those that could potentially be used for advanced plasma control (group 1b) and additional measurements that provide data for plasma evaluation and physics studies (group 2) [2]. This classification is made on the basis of the planned ITER operation scenario, which has three control levels: control of magnetic configuration, plasma kinetic control (n, T_e etc.) and fast plasma shutdown [3]. This paper examines the role of diagnostics in a few key areas. The ability of the diagnostic set to control the plasma shape, both using the magnetics and using the plasma position reflectometer [4] to provide estimates of the plasma-wall gaps to the control system is summarized. The technique proposed for control of the burn in [5] is refined by defining the diagnostics necessary for its implementation, and assessing the effect of introducing noise into the divertor radiation control loop. Finally, groupings of specific diagnostics from within the ITER set are proposed to provide inputs to the "state-cognizant" supervisory plasma control system, which maintains the plasma within the pre-set scenario during the ITER pulse.

2. Control of the plasma shape

The capabilities of the ITER PF control system have been extensively studied, and reported in [6]. In the absence of drifts, the ITER diagnostic coil set does not limit the performance of the control system [7]. For long pulses, where drifts are possible, it is planned to use a poloidally distributed reflectometry system. This can meet the 2 cm measurement accuracy target for individual gaps [8], but a method of re-initializing the magnetics prior to plasma ramp-down remains to be developed, and additional information is needed on the location of the strike points [4]. Figure 1 shows preliminary estimates of the reconstruction errors, and Figure 2 shows the error in determining global parameters using the reflectometer gaps and PF coil set currents as inputs. It appears that 8 reflectometers are adequate for basic shape control if placed near the control gaps, however ~14 are required to deduce the plasma current to 1% and to re-initialize the magnetics system prior to rampdown.
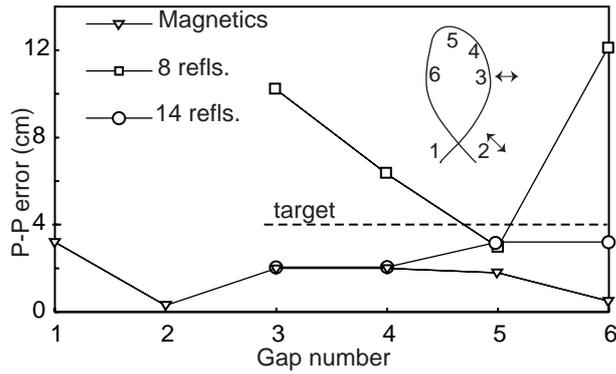
Figure 1: Typical reconstruction errors for magnetics [7] and position reflectometry (divertor strike points and Ip fixed and a_f varied).
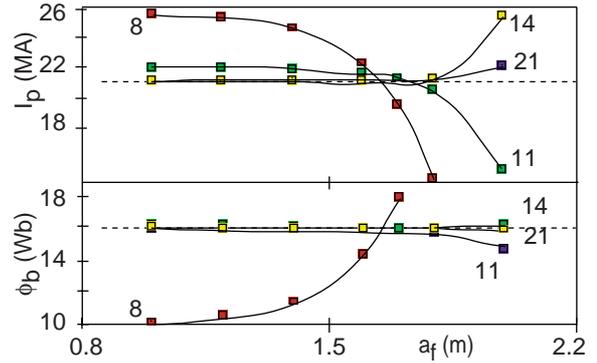

Figure 2: The variation of plasma current and boundary flux with filament minor radius, shown for reconstructions with 8,11,14 and 21 reflectometers [4].

3. Kinetic control of the burn

Previous tests of the model using the 1.5D PRETOR code [6,2,3], incorporating a 0D model of the divertor [9], assumed perfect measurements of the relevant input quantities, namely fusion power, volume average density, plasma state (L/H mode transition) and power reaching the divertor target, and showed that simultaneous control of the fusion power and divertor power load was possible. Figure 3 illustrates the kinetic control scenario, together with candidate diagnostics selected from the ITER diagnostic set. Unavoidably, these introduce time delays, noise, and systematic errors. For the neutron source monitors [10], it is expected that systematic errors will be < 10 %, the time response < 10 ms, and the noise < 5 %. For the toroidal interferometer/ polarimeter [11], systematic errors are expected to be < 3 %, the time response < 1 ms with noise < 1 %. For the IR thermography system, which is optimized for survey extent and compact optics, rather than S/N [12], systematic errors in T_{plate} from 230 ^{O}C upwards are expected to be less than 10 %, the time delay introduced is ~ 0.8 s (this is the 1/e response time of the surface temperature to a step change in heat load), and the noise at 230 ^{O}C and 50 ms time interval is ~10 %.

As a first step in assessing the effect of including the diagnostic limitations in the control loop, a model of the IR measurement was incorporated in the PRETOR code. For this purpose the strike width was assumed constant at 0.1 m, the divertor plate was modeled as a 0.02 cm thick CFC slab held at 140 ^{O}C on the coolant side, and a simple PD controller working on $\varepsilon = f ((T_{plate} - T_{set}) / T_{set})$ signal was used to control the incremental gas feed at each time step. For f, the function shown in Figure 4 was found to provide a stable operating point for small perturbations, and to minimise the response time to large perturbations without leading to radiative collapse of the core. Figures 5 and 6 show selected divertor, diagnostic and plasma parameters for a typical run. A full power heating pulse is used as a test perturbation at 150 s. A set point of 500 ^{O}C is used; in steady state this corresponds to ~ 5 MW/m^2, which was the target set in previous simulations. T_{plate} is constant to within 20 % during the burn phase and heating excursion, even though there is a short attached period where the power to the target exceeds 10 MW/m^2. At t = 400 s, the

divertor set temperature is reduced to 200 $^{\circ}$C in anticipation of the H mode termination (it cannot be decreased further without increasing Z_{eff} in the core to the point where the plasma "collapses" during the P_{α} ramp-down), which deposits ~ 0.7 GJ onto the divertor, briefly increasing the temperature to ~ 1000 $^{\circ}$C. At low T_{plate} the noise performance of the diagnostic is relatively poor; this can be seen in Figure 6 as noise on the gas feed rate, and the connection length (and feeds through to noise on core parameters in figure 3 because the Ar impurity transport to the core is assumed instantaneous in the model). The temperature behaviour is not altered significantly in tests with zero instrumental noise. Based on these results, the performance of this instrument is adequate for control purposes, although an improvement of S/N at low T_{plate} is desirable. More testing will be required as our modeling of divertor physics improves. Future simulations will include the effects of the noise in the fusion power measurement and line average density measurement, and the low pass filter delays.
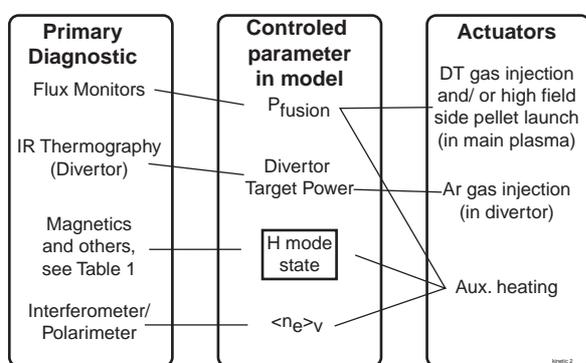

Figure 3: Schematic of the ITER kinetic control scenario. In the model, DT has injection was used used rather than pellet launch.
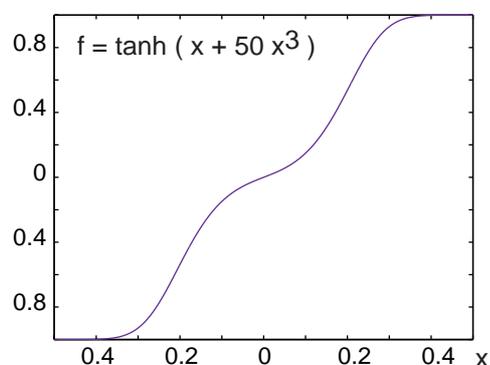

Figure 4: The function used to derive the error signal used to control the incremental Ar gas feed rate.
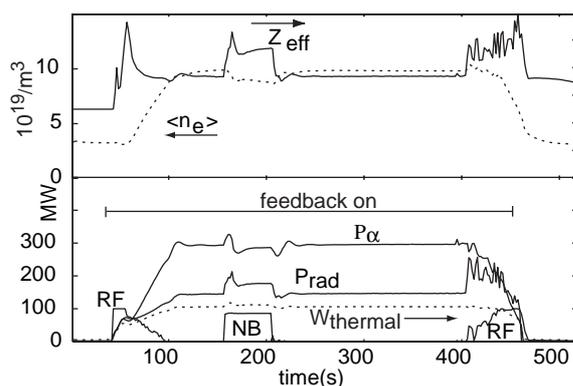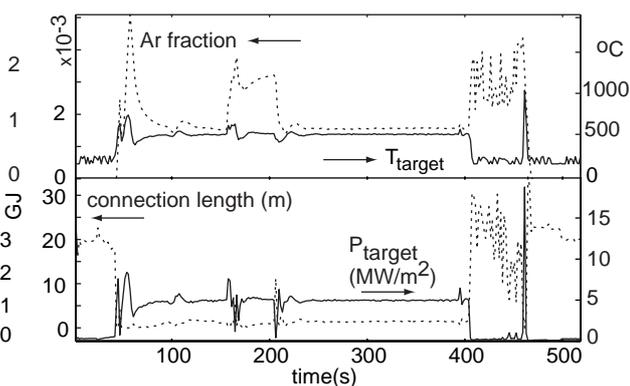

Figure 5: Selected model core parameters.

Figure 6: Selected model divertor parameters.

4. Determination of the plasma state

Figure 3 incorporates an example of a plasma state used as an input to the control system. In this case the magnetics and other diagnostics are used to determine whether the plasma is in H-mode or not. In practice multiple state indicators of this type will have to be produced in real time using a large fraction of the diagnostic set. Table 1 is a compilation of plasma state

indicators likely to be useful based on present knowledge, together with relevant diagnostic systems taken from the ITER diagnostic set in [2].

Table 1 : Some state indicators and corresponding diagnostics.

State	Indicator	Measurements (Diagnostics)
Confinement (L/H/VH/RS/ITB etc.)	H_H	τ_E (Magnetics), n_e core (LIDAR, reflectometry), T_e core (ECE, LIDAR),T_i (NPA, neutron cameras)
	Edge transport barrier, ELMs	n_e edge (Thomson scattering, reflectometry), T_e edge (Thomson scattering, ECE), D_α (D_α monitors), n_e fluctuations (reflectometry)
	Internal transport barrier	n_e core, T_e core, n_e fluctuations
	Shear reversal	q profile (Polarimeter, MSE, magnetics)
Pre-density limit	MARFE	Edge radiation (Bolometer arrays, Tangential IR/ Visible cameras, Visible continuum array), n_e poloidal asymmetry (Position reflectometry)
Pre-disruption	many	β (Magnetics), radiation (Bolometer arrays, Impurity monitors), mode formation (magnetics, reflectometry)
Neoclassical β limit	Significant NC tearing mode	mode formation, mode identification: m,n (magnetics) radial location (ECE, reflectometry), speed (magnetics, ECE, reflectometry)
Detached divertor	Flame front location	Divertor radiation (Bolometer arrays), J_{sat} at the plate (Langmuir probes), $T_{impurity}$ (spectroscopic arrays), n_e (divertor reflectometry), T_{plate} (IR thermography)
Runaway electron	$I_{runaway}$	Plasma current (Magnetics), Synchrotron emission (Tangential IR camera), γ emission (γ spectrometers) Cyclotron emission (ECE)

References
[1] A.E. Costley et al.: *in* Diagnostics for Experimental Thermonuclear Fusion Reactors. Plenum Press, New York, 1998, 41.
[2] V. Mukhovatov et al.: *ibid.* 25.
[3] J. Wesley et al.: Fusion Technology **32** (1997) 495
[4] N. Bretz et al.: *in* Diagnostics for Experimental Thermonuclear Fusion Reactors. Plenum Press, New York 1998, 129.
[5] D. Boucher et al.: in *Proc. 16th Int. Conf.* Montreal, 1996, **2**, (IAEA, Vienna 1997) 945.
[6] A. Portone et al.: Fusion Technol. **32** (1997) 374
[7] I. Senda and T.Shoji: Report on ITER Design Task D324, 1997 (*unpublished*)
[8] E.J. Doyle et al.: *in* Diagnostics for Experimental Thermonuclear Fusion Reactors. Plenum Press, New York 1998, 119.
[9] M. Sugihara et al.: J. Nucl. Mater. **241-243** (1997) 299
[10] C.W. Barnes et al.: in Diagnostics for Experimental Thermonuclear Fusion Reactors. Plenum Press, New York 1998, 479.
[11] T. Carlstrom et al.: *ibid.* 193.
[12] A. Herrmann et al. *ibid.* 569.